ACS Chemical Neuroscience

Letter

pubs.acs.org/chemneuro

Identification and Electrophysiological Evaluation of 2-Methylbenzamide Derivatives as $Na_v1.1$ Modulators

François Crestey,[§] Kristen Frederiksen,[§] Henrik S. Jensen,[§] Kim Dekermendjian,[§] Peter H. Larsen,[§] Jesper F. Bastlund,[§] Dunguo Lu,[†] Henry Liu,[†] Charles R. Yang,[†] Morten Grunnet,*[,§] and Niels Svenstrup*[,§]

[§]Neuroscience Drug Discovery, H. Lundbeck A/S, Ottiliavej 9, 2500 Valby, Denmark

[†]ChemPartner Co. Ltd., 998 Halei Road, Zhangjiang Hi-Tech Park, Shanghai 201203, P. R. China

Supporting Information

ABSTRACT: Voltage-gated sodium channels (Na_v) are crucial to the initiation and propagation of action potentials (APs) in electrically excitable cells, and during the past decades they have received considerable attention due to their therapeutic potential. Here, we report for the first time the synthesis and the electrophysiological evaluation of 16 ligands based on a 2-methylbenzamide scaffold that have been identified as $Na_v1.1$ modulators. Among these compounds, *N*,*N*′-(1,3-phenylene)bis(2-methylbenzamide) (**3a**) has been selected and evaluated in ex-vivo experiments in order to estimate the activation impact of such a compound profile. It appears that **3a** increases the $Na_v1.1$ channel activity although its overall impact remains moderate. Altogether, our preliminary results provide new insights into the development of small molecule activators targeting specifically $Na_v1.1$ channels to design potential drugs for treating CNS diseases.

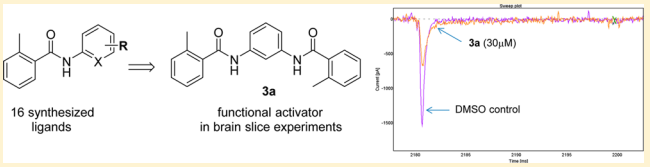

KEYWORDS: *2-Methylbenzamide derivatives, $Na_v1.1$ modulator, voltage-gated sodium channels, brain slices, fast-spiking interneurons*

Voltage-gated sodium channels[1] play a pivotal role in initiating and propagating action potentials (APs) in neurons, myocytes and endocrine cells.[2] Thus, Na^+ channels have been the focus of a vast body of research including drug discovery activities.[3] Indeed, various sodium channel inhibitors have successfully been developed as human drugs and are currently approved for treating a variety of indications such as pain, epilepsy, migraine, bipolar disorders, and cardiac arrhythmia.[4] By contrast, sodium channel activators are also known but have not previously been considered relevant in therapeutic settings mostly due to a high perceived risk of toxicity and convulsions. It has been clearly established that sodium channels play an important role in neuronal excitability by initiation and propagation of APs.[5] Interestingly, $Na_v1.1$ comprises the vast majority of the sodium current in GABAergic fast-spiking inhibitory interneurons that are immunoreactive for parvalbumin. Furthermore, it plays only a modest role in excitatory neurons due to the high redundancy of other types of sodium channels in these cells. Moreover, mouse models of reduced $Na_v1.1$ channel expression have revealed several phenotypes such as autistic-like behaviors, cognitive deficits, severe epilepsy, and unexpected death. Accordingly, it has been well recognized that an important number of diseases, especially Dravet syndrome, are closely related with loss of function mutations in $Na_v1.1$ channels.[6] Jensen and co-workers recently published that selective activators of the $Na_v1.1$ sodium channel may hold therapeutic potential within diseases such as epilepsy, schizophrenia and Alzheimer's disease.[7] Different classes of nonselective sodium channel activators are well-known including the pyrethroid insecticides exemplified by allethrin and deltamethrin, the steroid-like alkaloid-based toxins veratridine and batrachotoxin, as well as a number of peptide-toxins isolated from diverse organisms such as spiders, scorpions and sea anemones.[8] From a drug discovery perspective nonselective Na^+ channel activators are considered nonviable due to general overall neuronal activation introducing a state of hyperexcitability and thereby a number of epileptogenic related adverse effects. Some degree of selectivity is therefore a likely prerequisite for bringing a Na^+ channel activator to the market. So far, no claims or descriptions have been made for specific $Na_v1.1$ activators.

In order to identify such activators, a high-throughput screening (HTS) of a small-molecule library (~55 000 compounds) has been performed at a single concentration (30 μM) using a voltage protocol and veratridine and mexiletine as assay controls. Several derivatives having a 1,3-diamidobenzene core[9] and even more precisely containing a 2-methylbenzamide moiety were identified and confirmed as hits. Herein, we wish to present the design of 16 ligands bearing a 2-methylbenzamide unit in order to study the structure−activity relationship (SAR) of such a compound class as well as their electrophysiological evaluation on a HEK cell line with stable expression of $Na_v1.1$ channels. Furthermore, derivative **3a** was selected for brain slice experiments in order to understand the overall impact of the compound profile.

Published: June 26, 2015

DOI: 10.1021/acschemneuro.5b00147
ACS Chem. Neurosci. 2015, 6, 1302−1308

Scheme 1. Synthesis of Phenylamide 2, Diamides 3a–i, and Sulfonamide 3j[a]

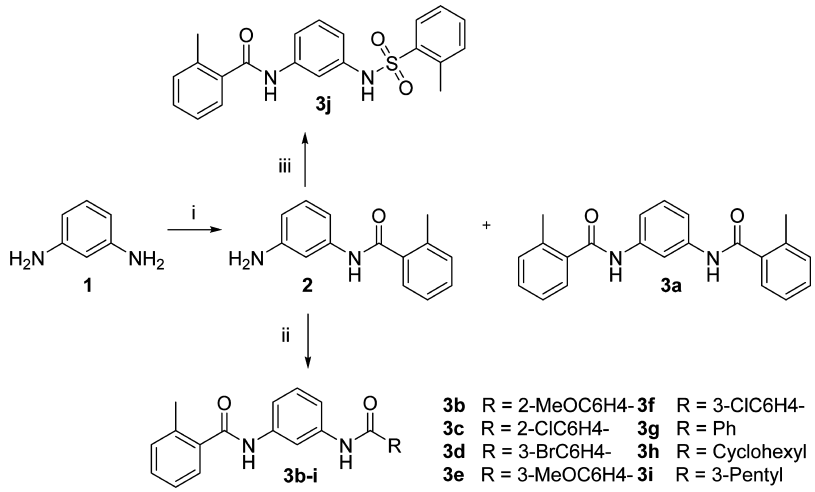

[a]Reagents and conditions: (i) 2-MePhCOCl (1 equiv), TEA (1.05 equiv), DCE, 0 °C to rt, **2**: 45%, **3a**: 35%; (ii) RCOCl (1.05 equiv), TEA (1.1 equiv), DCE–DCM (5:1), 0 °C to rt, **3b**: 83%, **3c**: 91%, **3d**: 96%, **3e**: 97%, **3f**: 96%, **3g**: 99%, **3h**: 99%, **3i**: 97%; (iii) 2-MePhSO$_2$Cl (1.05 equiv), TEA (1.1 equiv), dry THF, 0 °C to rt, 89%.

Scheme 2. Synthesis of Ester 3k, Diamides 3l–n, Tetrazole 3o, and Indoline 3p[a]

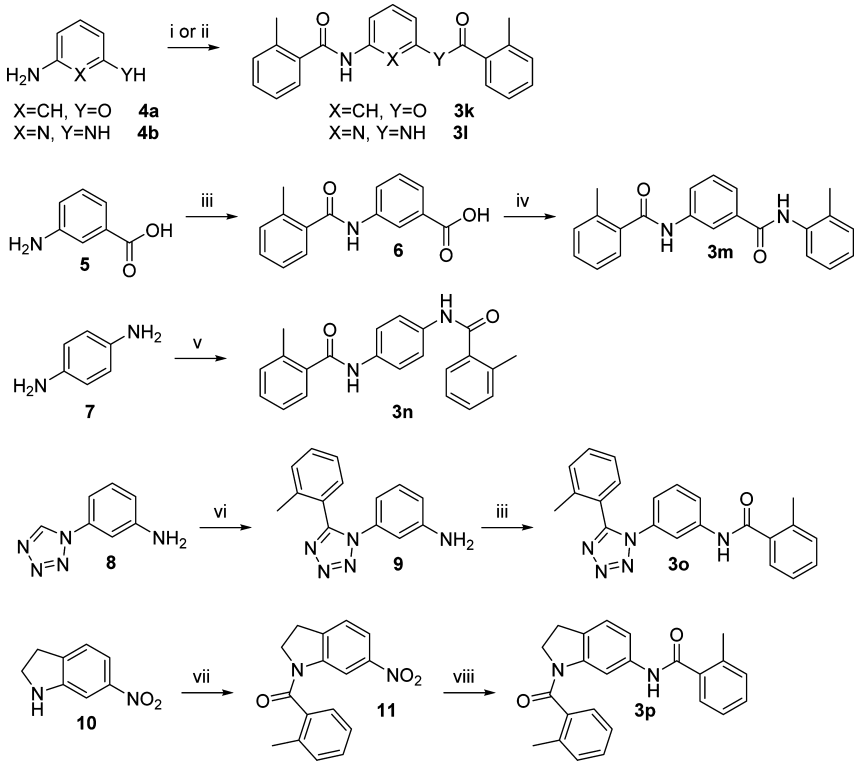

[a]Reagents and conditions: (i) 2-MePhCOCl (2.05 equiv), TEA (2.1 equiv), DMAP (0.04 equiv), DCE–DCM (5:1), 0 °C to rt, **3k**: 89%; (ii) 2-MePhCOCl (2.05 equiv), TEA (2.1 equiv), DCE–DCM (5:1), 0 °C to rt, **3l**: 66%; (iii) 2-MePhCOCl (1.05 equiv), TEA (1.1 equiv), $CHCl_3$, rt, **6**: 82%; **3o**: 87%; (iv) 2-MePhNH$_2$ (1.5 equiv), TEA (1.05 equiv), HATU (1 equiv), dry DMF, rt, 58%; (v) 2-MePhCOCl (2.1 equiv), TEA (2.2 equiv), DCE–DCM (8:3), 0 °C to rt then to 50 °C, 94%; (vi) 2-MePhI (1.1 equiv), Cs_2CO_3 (1.1 equiv), CuI (1 equiv), Pd(OAc)$_2$ (0.05 equiv), (*o*-furyl)$_3$P (0.1 equiv), dry CH_3CN, 65 °C then 90 °C, 16%; (vii) 2-MePhCOCl (1.05 equiv), TEA (1.1 equiv), dry THF, 0 °C to rt, 91%; (viii) (a) K_2CO_3 (3 equiv), $Na_2S_2O_4$ (6 equiv), NMP–EtOH (5:7), 0 to 100 °C; (b) 2-MePhCOCl (1.05 equiv), TEA (1.1 equiv), $CHCl_3$, 0 °C to rt, 23% over two steps.

CHEMISTRY

The synthetic pathway to obtain 2-methylbenzamide derivatives **3a–j** is outlined in Scheme 1. Benzene-1,3-diamine **1** reacted with one equivalent of 2-methylbenzoyl chloride in the presence of triethylamine (TEA) to furnish phenylamine **2** and bisbenzamide **3a** in 45% and 35% yields, respectively. Treatment of **2** with the appropriate acyl chlorides in a mixture of DCE–DCM provided the corresponding bis-benzamide derivatives **3b–i** in 83–99% yields.[10] Similarly, sulfonamide analogue **3j** was

DOI: 10.1021/acschemneuro.5b00147
ACS Chem. Neurosci. 2015, 6, 1302–1308

obtained from the reaction of **2** with 2-methylbenzenesulfonyl chloride in 89% yield.

The reaction sequence depicted in Scheme 2 was used as a convenient route to the compounds **3k−n**. After treatment of aminophenol **4a** with 2-methylbenzoyl chloride in the presence of TEA and a catalytic amount of DMAP ester **3k** was isolated in 89% yield. Following a similar protocol as above, aminopyridine **4b** and benzene-1,4-diamine **7** led to benzamide derivatives **3l** and **3n** in 66% and 94% yields, respectively. Finally, the diamide derivative **3m** was synthesized in a two-step protocol: aminobenzoic **5** was first acylated providing carboxylic acid **6** in 82% yield. Subsequently, amidation with *o*-toluidine, HATU as coupling reagent and TEA in dry DMF gave **3m** in 58% yield. In addition to the series of the 14 ligands detailed above, amide derivative **3o** was prepared in two steps in which one of the usual 2-methylbenzamide moieties was replaced by a tetrazole amide-bioisostere. Thus, tetrazole **8** furnished after C−H activation aniline **9** in 16% yield which was subsequently acylated to lead to tetrazole **3o** in 87% yield. Moreover, constrained analogue **3p** was prepared in a three-step procedure in order to test how the introduction of conformational restraint to a moderately flexible lead molecule would influence the activating properties with regards to the $Na_v1.1$ channel. Thus, nitroindoline **10** was first acylated furnishing amide **11** after which the nitro group was reduced with a slight excess of $Na_2S_2O_4$ in the presence of K_2CO_3. Subsequent acylation of the resulting intermediate with 2-methylbenzoyl chloride afforded indoline **3p** in 21% yield over three steps (Scheme 2).

RESULTS AND DISCUSSION

To obtain a thorough biological understanding and reconfirmation of hits identified during the primary screen, various electrophysiological approaches were pursued. Since the primary screen was performed in an automated setting (Ion Works/Barracuda) that does not allow for electrophysiological experiments in a quality that can match manual patch clamp with giga seals, the first experiment was to confirm the hits under conditions where a true giga seal can be obtained between the cell and the recording pipet.[11] This condition allows for a very precise determination, or clamp, of the cell membrane that can subsequently be controlled. Especially for ion channels that conduct large amount of currents and in addition show fast activation and inactivation kinetics, like voltage-gated Na^+ channels, reliable continuous control of the membrane potential is a prerequisite to fully characterize compound interactions with the channel. As an alternative to manual patch clamp experiments the automated Q-patch was applied where it is also possible to obtain giga ohm seals comparable to manual patch clamp.[12] $Na_v1.1$ channels, stable expressed in HEK cells, were activated by depolarizing voltage steps from −120 to +70 mV in 10 mV increments to obtain current−voltage (I−V) curves showing the expected voltage dependent activation revealed as an inward current deflection followed by fast inactivation as demonstrated in Figure 1. For more detailed compound evaluation, a more simple protocol was applied, that is, with only six voltage steps from −40 to +10 mV (with 10 mV increments). Each depolarizing step was activated from −120 mV and lasted for 20 ms and was separated with 500 ms. A holding potential (V_{hold}) of −80 mV was used between each protocol with six voltage steps (see Figure 2). A modulator of the $Na_v1.1$ channels can exert its action in a number of ways and the most relevant mode of action and associated electrophysiological profile for obtaining biological activity is at present unknown. We chose to focus on (1) impact on peak current, (2) total area under the curve (AUC) for the time duration of the depolarizing pulse, and (3) the compound's ability to decrease inactivation velocity. The later parameter is addressed by determining the tau value of the inactivation current decay. In this setting a slowing of the inactivation, and thereby more conducted current, is revealed by an increase in the tau value. As summarized in Table 1, compounds **3a**, **3c−j**, **3l**, **3n**, and **3p** from this 2-methylbenzamide family had a profile with a reduced peak current, but a compromised inactivation revealed as an increased tau value. As an example, peak current, AUC, and tau values (in %) relative to control at −10 mV for benzamide **3a** were 52, 81, and 124, respectively (see Figure 3). Unfortunately, no clear picture appeared with respect to the substitution pattern on the aromatic ring. However, ortho- and meta-substituted rings **3a** and **3c−f**, unsubstituted ring compound **3g**, derivatives bearing aliphatic moieties **3h−i**, sulfonamide **3j**, pyridine derivative **3l**, 1,4-substituted benzamide **3n**, and constrained indoline **3p** did provide novel active analogues displaying a noteworthy trend for this class of compounds: the total AUC was significantly reduced but much less than the peak current while the tau value was

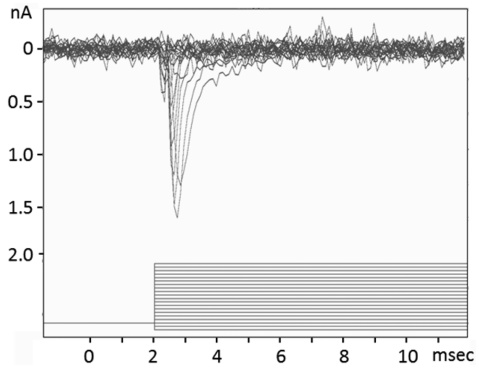

Figure 1. $Na_v1.1$ channels stable expressed in HEK cells were activated by stepping the membrane potential from −120 to +70 mV in 10 mV steps from a holding potential of −100 mV. Raw data traces. Traces measured on the Q-patch in single hole mode.

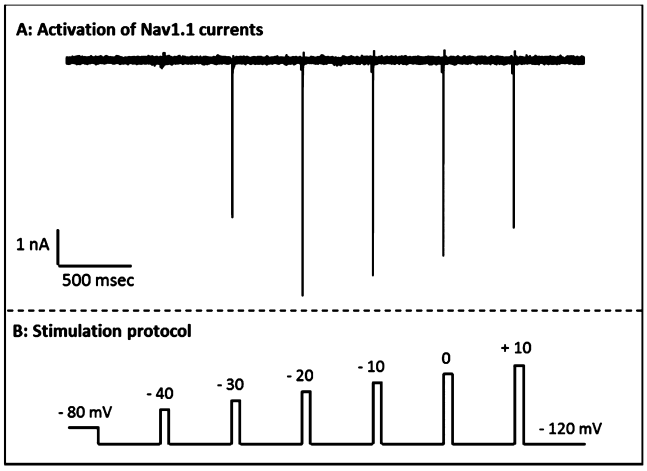

Figure 2. Screening protocol. $Na_v1.1$ channels stable expressed in HEK cells were activated by stepping the membrane potential from −120 mV in steps with 10 mV increments from −40 to +10 mV. Screening of test compounds was performed by evaluation of the effect induced by test compounds at −10 mV on the peak, AUC, and tau values. V_{hold} between the step protocol was −80 mV. Traces were measured on the Q-patch in single hole mode.

DOI: 10.1021/acschemneuro.5b00147
ACS Chem. Neurosci. 2015, 6, 1302−1308

Table 1. Peak Current, AUC, and Tau Values for Compounds 3a–p Tested at 30 μM on a HEK Cell Line with Stable Expression of $Na_v1.1$ Channels

		response in % (±SEM) relative to control at −10 mV[a]		
compd	n^b	peak (%)	AUC (%)	tau (%)
DMSO[c]	13	101 ± 1	102 ± 2	102 ± 2
3a	10	52 ± 2	81 ± 9	124 ± 6
3b	5	89 ± 1	100 ± 5	101 ± 4
3c	8	70 ± 5	83 ± 3	115 ± 3
3d	11	47 ± 3	81 ± 5	143 ± 7
3e	3	54 ± 3	86 ± 2	127 ± 8
3f	9	39 ± 2	51 ± 2	136 ± 14
3g	12	56 ± 3	83 ± 6	128 ± 3
3h	3	51 ± 1	74 ± 13	128 ± 4
3i	7	75 ± 2	93 ± 4	110 ± 6
3j	3	57 ± 2	70 ± 11	123 ± 6
3k	4	86 ± 2	92 ± 4	104 ± 6
3l	4	50 ± 12	80 ± 13	140 ± 11
3m	5	93 ± 1	96 ± 8	103 ± 10
3n	10	105 ± 1	112 ± 3	110 ± 2
3o	3	88 ± 2	86 ± 3	95 ± 2
3p	5	96 ± 2	112 ± 10	116 ± 9

[a]Performed at 30 μM. [b]Number of individual experiments. [c]DMSO control run on the same plates as the tested compounds.

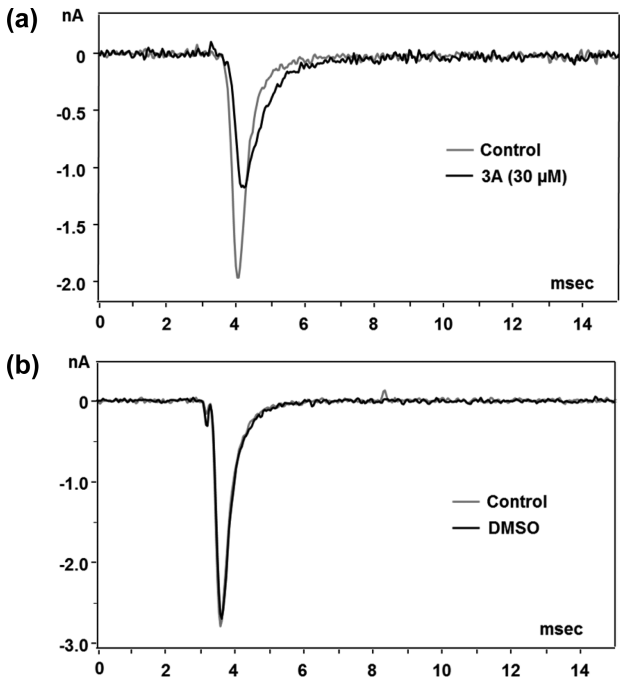

Figure 3. Effect of compound **3a** at 30 μM on the current trace activated to −10 mV. **3a** showed inhibition of the peak current and the AUC, but **3a** also induced a decrease in the inactivation (tau value) (see also Table 1). Control (gray trace) and compound **3a** (black trace) are shown in (A). For comparison control trace and time matched DMSO trace is shown in (B). DMSO did not induce any effect either on peak, AUC, or tau (see also Table 1).

considerably increased. Tetrazole **3o**, ester **3k**, and amide **3m** were nearly inactive with no noticeable effects on the three parameters of our designed electrophysiological protocol (see Table 1 for more details).

Voltage-gated sodium channels share high similarities of sequence, large expression in neurons (except $Na_v1.4$ which is expressed mainly in skeletal muscle and $Na_v1.5$ which is found primarily in cardiac muscle), and biophysical characteristics.[13] In order to quantify the selectivity profile of the compounds, the same electrophysiological protocol described above was applied using benzamide **3a** on $Na_v1.2$, -1.4, -1.5, -1.6, and -1.7 channels, stably expressed in HEK cells. As depicted in Table 2, peak values were significantly less reduced and tau values were significantly lower while the AUC values remained almost constant when compared with the values obtained for $Na_v1.1$ channel. In addition, intrinsic hepatic clearances (Cl_{int}) of eight synthesized compounds were also estimated for both rat and human after incubation of the corresponding compound in rat or human liver microsomes; apart from derivative **3p**, $Cl_{int,rat}$ and $Cl_{int,human}$ were relatively high with values between 3 and 38 L/kg/h (rat) and between 0.9 and 6.3 L/kg/h (human), respectively. Moreover, PgP efflux and permeability was investigated for a selection of compounds in the MDR1-MDCK cell assay. MDCK ratios[14] of derivatives **3a**, **3c**, **3d**, and **3l** were 0.45, 0.52, 0.31, and 0.64, respectively, showing that this class of compounds has a small or modest efflux ratio (see the Supporting Information for more details).

Table 2. Peak Current, AUC, and Tau Values for Compound 3a Tested at 30 μM on HEK Cell Lines with Stable Expression of $Na_v1.1$, -1.2, -1.4, -1.5, -1.6, and -1.7 Channels

		response in % (±SEM) relative to control at −10 mV[a]		
	n^b	peak (%)	AUC (%)	tau (%)
$Na_v1.1$	10	52 ± 2	81 ± 9	124 ± 6
$Na_v1.2$	4	71 ± 2	79 ± 2	97 ± 2
$Na_v1.4$	5	94 ± 5	79 ± 3	85 ± 5
$Na_v1.5$	4	82 ± 4	84 ± 6	102 ± 5
$Na_v1.6$	4	101 ± 6	98 ± 5	96 ± 1
$Na_v1.7$	4	93 ± 6	75 ± 2	84 ± 2

[a]Performed at 30 μM. [b]Number of individual experiments.

The biological nature of a compound profile as described above is difficult to predict. To gain more insight into whether an overall inhibitory, neutral or activation impact of these compounds was prevailing, ex vivo experiments with rat brain slices were performed (see Supporting Information for more details). In brief, whole cell patch clamp were performed on parvalbumin containing interneurons with basket cell appearance in the hippocampal pyramidal cell layer. As illustrated in Figure 4A, cells were initially challenged by ramps starting with resting membrane potentials from −70 mV that were gradually depolarized. The experiments were performed in the absence (control) and presence of $Na_v1.1$ modulator **3a** and as summarized data in Figure 4B application of **3a** shifted the threshold for firing APs to a more negative value. The reason for this is believed to be the activation of $Na_v1.1$ channels that facilitate the neuron to generate APs. To obtain a more thorough evaluation of the $Na_v1.1$ modulators ability to modify interneuron firing frequency depolarizing steps with different amplitude were provided to the neuron to provoke APs (see Figure 4C). As observed, **3a** was able to increase the number of evoked APs even though the effect was most prominent after weak depolarizations that render a larger window available for further activity increase. Data for application at 30 and 100 μM of benzamide **3a** are depicted in Figure 4D. For input–output and threshold experiments, a number of time

DOI: 10.1021/acschemneuro.5b00147
ACS Chem. Neurosci. 2015, 6, 1302–1308

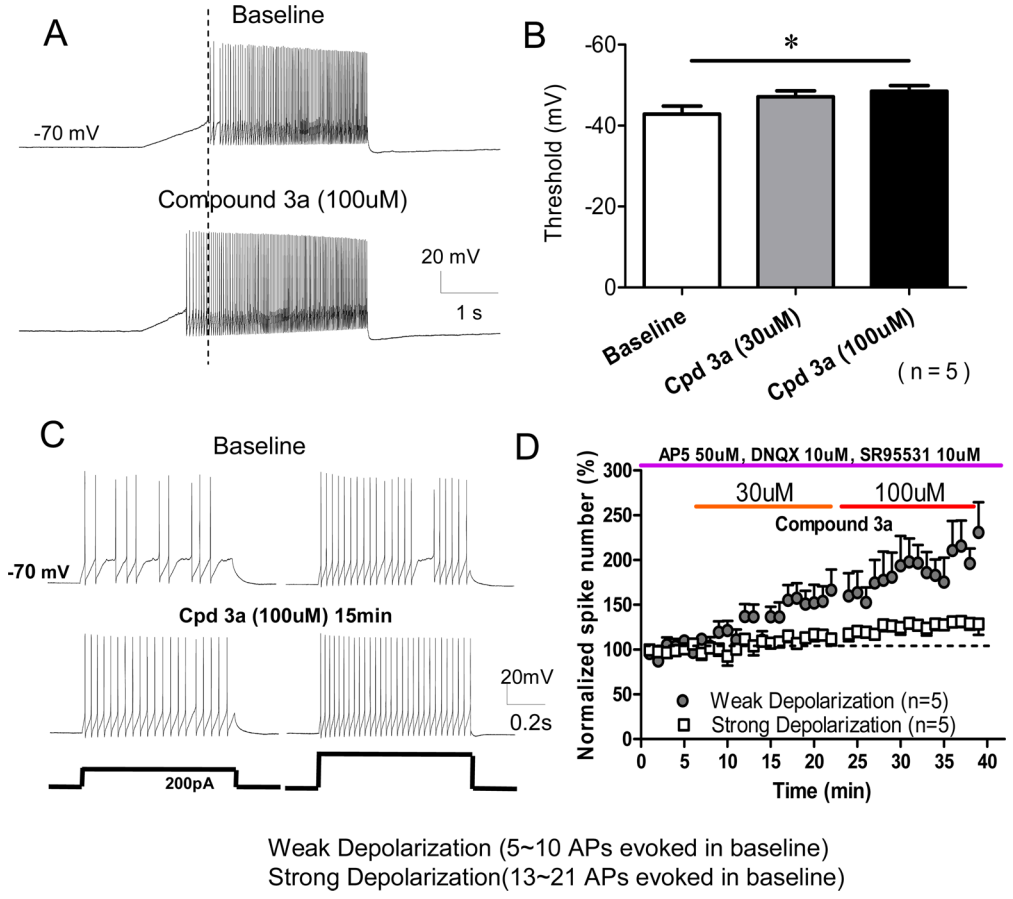

Figure 4. Compound **3a** increases neuronal excitability in a fast-spiking interneuron recorded in the stratum pyramidal in hippocampal CA1 field. (A) Top: Current ramp evoked repetitive spike firing in the baseline predrug period. Bottom: Following perfusion of **3a** (100 μM) for 10 min, the same current ramp now induced firing at a more negative membrane potential. V_{hold} = −70 mV. (B) Group data from five interneurons tested showed that **3a** was able at 100 μM (but not at 30 μM) to elicit firing at a more negative membrane potential, suggesting that **3a** lowers the threshold for firing. (C) Left top and bottom: Raw voltage traces recorded from an interneuron showed the evoked firing by a *weak* (200 pA) rectangular pulse before and after perfusion of **3a**. It was able to increase the excitability of the interneuron. Right top and bottom: baseline firing evoked by a *stronger* depolarizing pulse was also enhanced by **3a**. (*Weak* depolarization is defined as the depolarizing pulses used that evoked 5−10 spikes, and *strong* depolarization is defined as the depolarizing pulses used that evoked 13-21 spikes). (D) Time course of neuronal excitability change in five interneurons following **3a** perfusion. Note that **3a** (at 30 and 100 μM) can induce more firing of interneurons evoked by a weak current pulse than from a stronger current pulse. See the Supporting Information for more details.

matched control was performed to make certain that the observed effects were not due to sliding baseline as a function of time (data not shown).

To enable correct identification of fast-spiking parvalbumin expressing interneurons, some electrophysiological experiments were performed with biocytin in the pipet. After successful recordings biocytin, was injected into the cell and the slice was fixed for later identification. Slices were then costained for biocytin and parvalbumin to confirm that the compound had actually exerted its effect at a parvalbumin expressing interneuron (seethe Supporting Information for more details).

CONCLUSIONS

In summary, we have discovered novel 2-methylbenzamide derivatives that act as $Na_v1.1$ modulators. Among them, 2-methylbenzamide derivative **3a** has been demonstrated in ex vivo experiments to act as a functional activator of fast-spiking hippocampal interneurons. Even though its overall activation impact was moderate, addition of **3a** clearly resulted in an increase of interneuron activity. These preliminary yet promising results open up a novel and challenging area of investigations on pharmacological activators of $Na_v1.1$ channels, since such compound may have important therapeutic potential in the treatment of various CNS diseases. Further studies concerning discovery of subtype selective small molecule activators of the $Na_v1.1$ channel are currently in progress in our laboratories.

METHODS

1.1. Chemistry: Materials and Methods. Starting materials and reagents were obtained from commercial suppliers and used without further purification. Syringes which were used to transfer anhydrous solvents or reagents were purged with nitrogen prior to use. Yields refer to isolated compounds estimated to be >95% pure as determined by ^{1}H NMR and LC−MS. Thin-layer chromatography (TLC) was carried out on silica gel 60 F_{254} plates from Merck (Germany). Visualization was accomplished via UV lamp (254 nm). Flash column chromatography was performed on chromatography grade, silica 60 Å particle size 35−70 μm from Fisher Scientific using the solvent system as stated. Melting points were determined on a Büchi apparatus and are uncorrected. HRMS was performed on a Bruker MicroTOF instrument. ^{1}H NMR spectra were recorded on a Bruker 600-Avance-III spectrometer equipped with a 5 mm TCI cryoprobe operating at 600 MHz using $CDCl_3$ or DMSO-d_6 as solvents and TMS as internal standard. Coupling constants (J values) are given in hertz (Hz). Multiplicities of ^{1}H NMR

DOI: 10.1021/acschemneuro.5b00147
ACS Chem. Neurosci. 2015, 6, 1302−1308

signals are reported as follows: s, singlet; d, doublet; dd, doublet of doublets; t, triplet; dt, doublet of triplet; tt, triplet of triplets; ddd, doublet of doublet of doublets; m, multiplet; br, broad signal. LC−MS data were obtained on a PE Sciex API150EX instrument equipped with an ion-spray source and Shimadzu LC-A/SLC-10A LC system: column, 30 mm × 4.6 mm Waters Symmmetry C18 column with 3.5 μm particle size; solvent system, A = water−TFA (100:0.05) and B = water−acetonitrile−TFA (5:95:0.03) (TFA = trifluoroacetic acid); method, linear gradient elution with 90% A to 100% B in 2.4 min and then 10% B in 0.4 min, with a flow rate of 3.3 mL/min. Total time including equilibration was 2.8 min. Injection volume was 10 μL from a Gilson 215 autosampler.

1.2. Synthesis and Analytical Data of Representative Compounds. *3-Methoxy-N-(3-(2-methylbenzamido)phenyl)-benzamide* ***3e***. To a solution of phenylamide **2** (143 mg, 0.63 mmol, 1 equiv) in a mixture DCE−DCM (5:1, 12 mL) at room temperature was added TEA (97 μL, 0.70 mmol, 1.1 equiv). The reaction mixture was cooled to 0 °C, and 3-methoxybenzoyl chloride (93 μL, 0.66 mmol, 1.05 equiv) was added dropwise over 1 min. After a few minutes, the reaction mixture was allowed to warm up to room temperature and was stirred at this temperature for 2 h and concentrated in vacuo. The crude material was purified by column chromatography on silica gel using a gradient elution (EtOAc−heptane, 1:1 to 3:2) to afford diamide **3e** (222 mg, 97%) as a white solid. R_f = 0.54 (EtOAc−heptane, 1:1); mp 163.9−165.6 °C. ^{1}H NMR (600 MHz, DMSO-d_6): δ 10.35 (br s, 1H), 10.16 (br s, 1H), 8.27−8.34 (m, 1H), 7.50−7.57 (m, 3H), 7.43−7.47 (m, 2H), 7.37−7.42 (m, 2H), 7.28−7.33 (m, 3H), 7.16 (ddd, J = 8.2 and 2.6 and 0.9, 1H), 3.84 (s, 3H), 2.39 (s, 3H). LC−MS (m/z) 361.3 (MH^+). RT = 0.70. Purity (UV, ELSD): 100%; 100%. HRMS $C_{26}H_{32}N_3O_3$ [M + $H_2NEt_2^+$] calcd 434.2438, found 434.2440.

N,N′-(Pyridine-2,6-diyl)bis(2-methylbenzamide) ***3l***. To a solution of aminopyridine **4b** (400 mg, 3.67 mmol, 1 equiv) in a mixture DCE−DCM (5:1, 48 mL) at room temperature was added TEA (1.07 mL, 7.70 mmol, 2.1 equiv). The reaction mixture was cooled to 0 °C, and 2-methylbenzoyl chloride (0.98 mL, 7.51 mmol, 2.05 equiv) was added dropwise over 3 min. After a few minutes, the reaction mixture was allowed to warm up to room temperature and was stirred at this temperature for 22 h and concentrated in vacuo. The crude material was purified by column chromatography on silica gel using a gradient elution (EtOAc−heptane, 3:5 to 3:4) to afford the desired diamide **3l** (840 mg, 66%) as a colorless oil which slowly crystallized as a white solid when stored in the fridge overnight. R_f = 0.44 (EtOAc−heptane, 3:5). ^{1}H NMR (600 MHz, DMSO-d_6): δ 10.51 (s, 2H), 7.79−7.93 (m, 3H), 7.41−7.48 (m, 2H), 7.38 (dt, J = 7.5 and 1.3, 2H), 7.23−7.32 (m, 4H), 2.39 (s, 6H); LC−MS (m/z) 346.1 (MH^+). RT = 0.73. Purity (UV, ELSD): 96%; 100%. HRMS $C_{25}H_{31}N_4O_2$ [M + $H_2NEt_2^+$] calcd 419.2442, found 419.2453.

N,N′-(1,4-Phenylene)bis(2-methylbenzamide) ***3n***. To a solution of benzene-1,4-diamine **7** (450 mg, 4.16 mmol, 1 equiv) in a mixture DCE−DCM (8:3, 22 mL) at room temperature was added TEA (1.27 mL, 9.15 mmol, 2.2 equiv). The reaction mixture was cooled to 0 °C, and 2-methylbenzoyl chloride (1.14 mL, 8.74 mmol, 2.1 equiv) was added dropwise over 2 min. After a few minutes, the reaction mixture was allowed to warm up to room temperature and was stirred at this temperature for 1.5 h then at 50 °C for 1 h. The resulting mixture was cooled to room temperature and filtered. The resulting precipitate was washed successively with DCM, DCE, and water then freeze-dried overnight to afford the desired diamide **3n** (1.35 g, 94%) as a white solid. R_f = 0.52 (EtOAc−heptane, 1:1). ^{1}H NMR (600 MHz, DMSO-d_6): δ 10.28 (s, 2H), 7.70 (s, 4H), 7.46 (d, J = 7.4, 2H), 7.39 (dt, J = 7.9 and 1.2, 2H), 7.26−7.33 (m, 4H), 2.38 (s, 6H); LC−MS (m/z) 345.3 (MH^+). RT = 0.69. Purity (UV, ELSD): 95%; 93%. HRMS $C_{26}H_{32}N_3O_2$ [M + $H_2NEt_2^+$] calcd 418.2489, found 418.2485.

1.3. Electrophysiology: Methods. A HEK cell line with stable expression of $Na_v1.1$ channels was used for in vitro electrophysiological recordings in patch clamp mode. $I-V$ curves for both activation and inactivation were performed in order to confirm the expected characteristic of $Na_v1.1$ channels, both with manual patch clamp and with automated patch clamp (Ion Works and Q-Patch). The first HTS screening of a small library was performed on the Ion Works platform, but the following evaluation of new compounds from medicinal chemistry efforts was performed with a Q-patch16x in single hole mode. It is possible to obtain gigaohm seals with the Q-patch, which make higher quality recordings more comparably to manual patch. For electrophysiological recordings, HEK cells were harvested with detachin (5−10 min) and applied to the Q-patch with a cell density between 1 and 3 million cells/mL. The cell suspension could be used up to 4−5 h after harvesting with good performance. For evaluation of the effects of compound on the peak current, AUC and tau values a protocol with six voltage steps were constructed. The voltage steps were depolarizing steps from −40 mV up to +10 mV (with 10 mV increments). Each depolarizing step was activated from −120 mV and lasted for 20 ms and was separated with 500 ms. A V_{hold} of −80 mV was used between each protocol with six voltage steps (Figure 2). The single protocol with six voltage steps was run approximately every minute. For tests of compounds in a single concentration, the voltage protocol was run six times in control (∼6 min) followed by drug application and six voltage runs in drug (∼6 min) and finally a wash out and six voltage runs again (∼6 min). Effects of compounds were measured relative to control values before drug application for each cell. For more details concerning all the cell lines, see the Supporting Information.

■ ASSOCIATED CONTENT

Supporting Information

Full experimental details for all synthesized compounds, ^{1}H and ^{13}C NMR spectra of selected compounds, brain slice experiments, and costaining protocols as well as table containing intrinsic clearance and MDCK ratio. The Supporting Information is available free of charge on the ACS Publications website at DOI: 10.1021/acschemneuro.5b00147.

■ AUTHOR INFORMATION

Corresponding Authors

*Phone: +45 3643 2421. E-mail: nisv@lundbeck.com.
*Phone: +45 3643 5173. E-mail: mgru@lundbeck.com.

Author Contributions

H.S.J., K.D., J.F.B., M.G., and N.S. conceived and designed the project. F.C. carried out the organic synthesis and analyzed all the compounds. K.F. carried out and analyzed the in vitro experiments. P.H.L. carried out and analyzed the costaining experiments. D.L., H.L., and C.Y. carried out and analyzed the ex vivo experiments. F.C., K.F., M.G., and N.S. wrote the manuscript with the help of D.L., H.L., and C.Y.

Notes

The authors declare no competing financial interest.

The authors thank the Danish National Advanced Technology Foundation for financial support (Grant 023-2011-3).

■ ACKNOWLEDGMENTS

The authors thank Peter Brøsen for HRMS measurements and Dr. Martin Carnerup for providing pharmacological data.

■ ABBREVIATIONS

DCM, dichloromethane; DCE, 1,2-dichloroethane; EtOAc, ethyl acetate; TEA, triethylamine; THF, tetrahydrofuran; DMAP, 4-dimethylaminopyridine; HATU, 1-[bis(dimethylamino)-methylene]-1*H*-1,2,3-triazolo[4,5-*b*]pyridinium 3-oxidhexa-fluorophosphate; DMF, *N*,*N*-dimethylformamide; NMP, *N*-methyl-2-pyrrolidone; AUC, area under the curve; MDCK, Madin−Darby canine kidney; CNS, central nervous system; AP, action potential; $I-V$, current−voltage; V_{hold}, holding potential; Cl_{int}, intrinsic hepatic clearance

DOI: 10.1021/acschemneuro.5b00147
ACS Chem. Neurosci. 2015, 6, 1302−1308

REFERENCES

(1) (a) Wood, J. N., and Baker, M. (2001) Voltage-gated Sodium Channels. *Curr. Opin. Pharmacol. 1*, 17−21. (b) Yu, F. H., and Catterall, W. A. (2003) Overview of the Voltage-gated Sodium Channel Family. *Genome Biol. 4*, 207.

(2) (a) Hodgkin, A. L., and Huxley, A. F. (1952) A Quantitative Description of Membrane Current and its Application to Conduction and Excitation in Nerve. *J. Physiol. 117*, 500−544. (b) Amstrong, C. M., and Hille, B. (1998) Voltage-gated Ion Channels and Electrical Excitability. *Neuron 20*, 371−380.

(3) (a) Taylor, C. P., and Narasimhan, L. S. (1997) Sodium Channels and Therapy of Central Nervous System Diseases. *Adv. Pharmacol. 39*, 47−98. (b) Goldin, A. L. (2001) Resurgence of Sodium Channel Research. *Annu. Rev. Physiol. 63*, 871−894. (c) England, S., and de Groot, M. J. (2009) Subtype-selective Targeting of Voltage-gated Sodium Channels. *Br. J. Pharmacol. 158*, 1413−1425. (d) Castle, N., Printzenhoff, D., Zellmer, S., Antonio, B., Wickenden, A., and Silvia, C. (2009) Sodium Channel Inhibitor Drug Discovery Using Automated High Throughput Electrophiysiology Platforms. *Comb. Chem. High Throughput Screening 12*, 107−122.

(4) For a review on voltage-gated sodium channel blockers in neurological and non-neurological diseases, see: Eijkelkamp, N., Linley, J. E., Baker, M. D., Minett, M. S., Cregg, R., Werdehausen, R., Rugiero, F., and Wood, J. N. (2012) Neurological Perspectives on Voltage-gated Sodium Channels. *Brain 135*, 2585−2612.

(5) (a) Catterall, W. A., Goldin, A. L., and Waxman, S. G. (2005) International Union of Pharmacology. XLVII. Nomenclature and Structure-Function Relationships of Voltage-gated Sodium Channels. *Pharmacol. Rev. 57*, 397−409. (b) Catterall, W. A. (2012) Voltage-gated Sodium Channels at 60: Structure, Function and Pathophysiology. *J. Physiol. 590*, 2577−2589.

(6) (a) Yu, F. H., Mantegazza, M., Westenbroek, R. E., Robbins, C. A., Kalume, F., Burton, K. A., Spain, W. J., McKnight, G. S., Scheuer, T., and Catterall, W. A. (2006) Reduced Sodium Current in GABAergic Interneurons in a Mouse Model of Severe Myoclonic Epilepsy in Infancy. *Nat. Neurosci. 9*, 1142−1149. (b) Ogiwara, I., Miyamoto, H., Morita, N., Atapour, N., Mazaki, E., Inoue, I., Takeuchi, T., Itohara, S., Yanagawa, Y., Obata, K., Furuichi, T., Hensch, T. K., and Yamakawa, K. (2007) $Na_v1.1$ Localizes to Axons of Parvalbumin-Positive Inhibitory Interneurons: A Circuit Basis for Epileptic Seizures in Mice Carrying an *Scn1a* Gene Mutation. *J. Neurosci. 27*, 5903−5914. (c) Guerrini, R. (2012) Dravet Syndrome: the Main Issues. *Eur. J. Paediatr. Neurol. 16* (Suppl. 1), S1−S4. (d) Han, S., Tai, C., Westenbroek, R. E., Yu, F. H., Cheah, C. S., Potter, G. B., Rubenstein, J. L., Scheuer, T., de la Iglesia, H. O., and Catterall, W. A. (2012) Autistic-like Behaviour in *Scn1a*$^{\pm}$ Mice and Rescue by Enhanced GABA-mediated Neurotransmission. *Nature 489*, 385−390. (e) Kalume, F., Westenbroek, R. E., Cheah, C. S., Yu, F. H., Oakley, J. C., Scheuer, T., and Catterall, W. A. (2013) Sudden Unexpected Death in a Mouse Model of Dravet Syndrome. *J. Clin. Invest. 123*, 1798−1808.

(7) Jensen, H. S., Grunnet, M., and Bastlund, J. F. (2014) Therapeutic Potential of $Na_v1.1$ Activators. *Trends Pharmacol. Sci. 35*, 113−118.

(8) (a) Otoom, S., Tian, L.-M., and Alkadhi, K. A. (1998) Veratridine-treated Brain Slices: A Cellular Model for Epileptiform Activity. *Brain Res. 789*, 150−156. (b) Miyawaki, T., Tsubokawa, H., Yokota, H., Oguro, K., Konno, K., Masuzawa, T., and Kawai, N. (2002) Differential Effects of Novel Wasp Toxin on Rat Hippocampal Interneurons. *Neurosci. Lett. 328*, 25−28. (c) Catterall, W. A., Cestèle, S., Yarov-Yarovoy, V., Yu, F. H., Konoki, K., and Scheuer, T. (2007) Voltage-gated Ion Channels and Gating Modifier Toxins. *Toxicon 49*, 124−141. (d) Soderlund, D. M. (2012) Molecular Mechanisms of Pyrethroid Insecticide Neurotoxicity: Recent Advances. *Arch. Toxicol. 86*, 165−181.

(9) A recent study showed a series of bis-amides as TASK-1-selective inhibitors. For more details, see: Flaherty, D. P., Simpson, D. S., Miller, M., Maki, B. E., Zou, B., Shi, J., Wu, M., McManus, O. B., Aubé, J., Li, M., and Golden, J. E. (2014) Potent and Selective Inhibitors of the TASK-1 Potassium Channel Through Chemical Optimization of a Bis-amide Scaffold. *Bioorg. Med. Chem. Lett. 24*, 3968−3973.

(10) Abdel-Aziz, M., Matsuda, K., Otsuka, M., Uyeda, M., Okawara, T., and Suzuki, K. (2004) Inhibitory Activities Against Topoisomerase I & II by Polyhydroxybenzoyl Amide Derivatives and Their Structure-activity Relationship. *Bioorg. Med. Chem. Lett. 14*, 1669−1672.

(11) A seal between the cell and recording pipet with very high resistance (1 GΩ or more) is called a giga seal.

(12) This has been evaluated with Na^+ channels to perform at a quality level comparable to manual recordings.

(13) Goldin, A. L., Barchi, R. L., Caldwell, J. H., Hofmann, F., Howe, J. R., Hunter, J. C., Kallen, R. G., Mandel, G., Meisler, M. H., Netter, Y. B., Noda, M., Tamkun, M. M., Waxman, S. G., Wood, J. N., and Catterall, W. A. (2000) Nomenclature of Voltage-gated Sodium Channels. *Neuron 28*, 365−368.

(14) Membrane permeability of selected derivatives was examined and obtained in an MDCK cell system expressing human MDR1 [ABCB1, P-glycoprotein (P-gp)] as previously described.[15]

(15) Blom, S. M., Rottländer, M., Kehler, J., Bundgaard, C., Schmitt, N., and Jensen, H. S. (2014) From Pan-Reactive K_v7 Channel Opener to Subtype Selective Opener/Inhibitor by Addition of Methyl Group. *PLoS One 9*, e100209.

DOI: 10.1021/acschemneuro.5b00147
ACS Chem. Neurosci. 2015, 6, 1302−1308